STRUCTURAL AND CHEMICAL VARIATION IN CHROMIUM CHLORITE

DAVIS M. LAPHAM,* *Columbia University, New York, New York.*

ABSTRACT

A detailed analysis of x-ray powder diffraction graphs of chromium chlorite yields evidence for chromium substitution between 0 per cent and 8 per cent Cr_2O_3 in both the octahedral and tetrahedral sites of the talc and brucite layers. "Comorphism" is suggested for this substitution of one element in two different structural positions.

X-ray powder diffraction measurements based on x-ray spectrographic analyses provide accurate determinations of total chromium content. Certain x-ray "d" spacings and intensity values correlate with Cr_2O_3 content, while others indicate the extent of octahedral or tetrahedral chromium substitution.

Indices of refraction increase almost linearly with chromium content, the octahedral and tetrahedral substitution curves having slightly different slopes which converge at approximately 2 per cent Cr_2O_3. A similar convergence is noted for x-ray powder and differential thermal data.

Below 2 per cent, there is no correlation of properties and chromium content, because the net effects are overcome by Fe substitutions for Mg. Thermal data indicates that the chromium chlorite structure may have either greater or lesser stability than the Fe-Mg chlorites. Thermal stability is inversely proportional to chromium content.

Chromium chlorites with more than 2 per cent Cr_2O_3 may be classified as kotschubeite (dominantly tetrahedral chromium) and kammererite (dominantly octahedral chromium). When the Cr_2O_3 content is less, a terminology analogous to the corundophilite-prochlorite-clinochlore-penninite grouping for the Fe-Mg chlorites may be used. The term "chromium chlorite" is a useful field term applicable to pink or rose-violet chlorite.

PART I. SYNOPSIS

INTRODUCTION

The research on which this paper is based, covering a period of three years, is devoted to the differentiation of members of the chromium chlorite group. Samples were collected from chromite localities in Pennsylvania. Specimens from the National Museum, Washington, D. C. were kindly loaned by Dr. George Switzer and the late Dr. W. F. Foshag. Additional samples were available from the research collection at Columbia University.

Optical, x-ray and thermal data have been combined with chemical analyses, x-ray spectrographic studies, and information on the general chlorite structure to develop a simple classification based both on the Si/Al ratio and the position of chromium substitution.

I extend my sincere appreciation to Professor Paul F. Kerr of Columbia University, under whose direction this project has been carried

* Present address: Bureau of Topographic and Geological Survey, Harrisburg, Pennsylvania.

out. Very fine specimens of chromium chlorite from Erzincan Province, Turkey were kindly sent to Professor Kerr by Mr. Raoul Bergman of the Mutual Chemical Company of America. Additional specimens from this province were supplied by Mr. James Hillebrand, Ouray, Colorado through Mr. Otto Kopp, Columbia University. The writer is also grateful to Dr. Hugo Steinfink, Shell Research Laboratory for permission to use his single crystal x-ray data, and to Mr. William A. Bassett for stimulating discussions on many phases of this work.

Chlorite Chemistry

As chromium is introduced into the general chlorite structure, corresponding variations occur in the relative amounts of other cations. Chemical analyses and x-ray spectrographic determinations have been used to determine chemical composition. Chemical analyses by W. H. Herdsman, analytical chemist, Glasgow, Scotland and other analyses from the literature have been coordinated with x-ray, optical, and differential thermal data. Published analyses have not, as a rule, been utilized in constructing standardization curves. Shannon's analysis (1920) of a chromium chlorite from Deer Creek, Wyoming was used as an end point for the chromium x-ray spectrographic curve. Gonyer's chromic oxide analysis (Ross, 1929) for #27 has also been used.

Table I includes six chemical analyses by W. H. Herdsman and Shannon's Deer Creek analysis, listed in order of increasing chromium content, from left to right. Silica is nearly constant throughout the range of chromium substitution from 0.10 per cent to 7.88 per cent Cr_2O_3. However, Al_2O_3 varies considerably, exhibiting a sharp decrease between 1.14 per cent and 6.47 per cent Cr_2O_3. The lack of a consistent relation between Al_2O_3 per cent and Cr_2O_3 per cent at a constant SiO_2 per cent suggests that chromium substitution is only indirectly related to aluminum content. CaO and MgO increase with increasing chromium content in a regular manner, representing an attempt at charge equalization, especially at high Cr_2O_3 percentages. High K_2O and Na_2O in the Zermatt chlorite tend to maintain charge neutrality. All analyzed material was carefully selected under a binocular microscope to eliminate impurities. X-ray patterns served as an additional check.

Theoretical specific gravities calculated from chemical analyses and unit cell dimensions are compared with specific gravities determined with a Berman balance in Table II. Specimen #27 from Webster, North Carolina was too fine-grained for accurate specific gravity measurements. Discrepancies greater than 0.01 may be attributed to chromite, mica, and/or vermiculite impurities, especially in #3 which is closely associated

TABLE I. CHEMICAL ANALYSES OF CHROMIUM CHLORITES

Sample	#4 Zermatt Valais, Switz.	#3 Chester Cy., Pa.	#9 Ogushi, Hizen, Japan	#2 West Chester, Pa.	#10 Siskiyou Cy., Calif.	#24 Erzin-can, Turkey	#11* Deer Creek, Wyo.
Oxide							
SiO_2	32.92	33.60	36.43	31.18	32.08	32.22	32.12
Al_2O_3	14.57	10.14	12.24	17.68	13.98	8.66	9.50
Fe_2O_3	2.31	8.42	0.94	1.88	0.42	0.46	—
Cr_2O_3	0.10	0.12	0.54	1.14	3.40	6.47	7.88
TiO_2	Trace	0.12	Trace	Trace	Trace	—	—
FeO	3.44	2.39	6.87	1.72	1.36	1.38	1.98
MgO	32.68	29.32	30.94	32.58	34.66	35.06	35.36
MnO	0.06	0.23	0.11	0.01	0.02	Trace	—
CaO	0.05	0.05	0.33	0.10	0.72	1.04	1.24
NiO	0.05	0.08	0.09	0.09	0.09	Nil	—
$H_2O-105°$	0.09	1.26	0.13	0.48	0.32	0.58	—
$H_2O+105°$	13.13	13.78	11.42	12.93	12.93	13.82	10.25
K_2O	0.15	Trace	Nil	Trace	Trace	—	—
Na_2O	0.52	0.53	Trace	0.14	Trace	—	—
Total	100.10	100.04	100.04	99.93	99.98	99.69	98.33

Analyses by W. H. Herdsman.
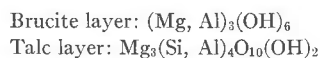* Analyses by E. V. Shannon (1920)
— Oxide not analyzed.
#9   U. S. National Museum #87144.
#10   U. S. National Museum #104723.
#11   U. S. National Museum #93908.

with vermiculite. Specific gravity tends to increase with increasing chromium content.

The schematic chemical composition of magnesian chlorite is as follows:

Brucite layer: $(Mg, Al)_3(OH)_6$
Talc layer: $Mg_3(Si, Al)_4O_{10}(OH)_2$

Chemical formulas based on the chemical analyses, given in Table III, were carried out on the basis of 18 oxygen atoms per unit cell, ten of which are bonded to metallic cations, and the remainder present as (OH). In accordance with the theoretical formula, the tetrahedral layer was filled first with Si, Al, Ti, and Cr to a total of four cations per unit cell. The remainder were placed in the octahedral position, with the exception of Ca, K, and Na, whose position is probably within the Si-O hexagonal

<div align="center">

TABLE II. COMPARISON OF THEORETICAL AND OBSERVED
SPECIFIC GRAVITY DETERMINATIONS

</div>

Sample	Theoretical Sp. Gr.	Observed Sp. Gr.
# 4	2.662	2.653
# 3	2.708	2.631
# 9	2.733	2.738
# 2	2.678	2.648
#10	2.619	2.622
#27*	2.637	—
#24	2.639	2.645
#11	2.747	2.718

* Analysis by Gonyer (Ross, 1929).

<div align="center">

TABLE III. CALCULATED FORMULAS OF CHROMIUM CHLORITES
FROM TABLE I

</div>

\# 4 Zermatt, Valais, Switzerland

$Na_{.13}K_{.02}Ca_{.005}(Mg_{4.53}Al_{.66}Fe^2_{.27}Fe^3_{.14}Cr_{.007}Mn_{.005}Ni_{.004})(Si_{3.06}Al_{.94})O_{10}(OH)_{8.11}$

$(Na,K,Ca,)_{.16}(Mg,Al,Fe^2,Fe^3,Cr,Mn,Ni)_{5.62}(Si,Al)_4O_{10}(OH)_{8.11}$

\# 3 Chester Co., Pennsylvania

$Na_{.13}Ca_{.005}(Mg_{4.07}Fe^3_{.59}Al_{.25}Fe^2_{.19}Mn_{.02}Cr_{.009}Ni_{.006})(Si_{3.13}Al_{.86}Ti_{.01})O_{10}(OJ)_{8.73}$

$(Na,Ca)_{.14}(Mg,Fe^3,Al,Fe^2,Mn,Cr,Ni)_{5.13}(Si,Al,Ti)_4O_{10}(OH)_{8.73}$

\# 9 Ogushi, Hizen, Japan

$Ca_{.04}(Mg_{4.57}Al_{1.04}Fe^2_{.57}Fe^3_{.07}Cr_{.04}Mn_{.01}Ni_{.01})(Si_{3.61}Al_{.39})O_{10}(OH)_{7.53}$

$Ca_{.04}(Mg,Al,Fe^2,Fe^3,Cr,Mn,Ni)_{6.31}(Si,Al)_4O_{10}(OH)_{7.53}$

\# 2 Chester, Pennsylvania

$Na_{.03}Ca_{.01}(Mg_{4.5}Al_{.82}Fe^2_{.13}Fe^3_{.13}Cr_{.08}Ni_{.007})(Si_{2.89}Al_{1.11})O_{10}(OH)_{8.28}$

$(Na,Ca)_{.04}(Mg,Al,Fe^2,Fe^3,Cr,Ni)_{5.66}(Si,Al)_4O_{10}(OH)_{8.28}$

\#10 Siskiyou Co., California

$Ca_{.07}(Mg_{4.64}Al_{.62}Fe^2_{.1}Fe^3_{.03}Ni_{.006}Mn_{.001})(Si_{2.9}Al_{.86}Cr_{.24})O_{10}(OH)_{7.97}$

$Ca_{.07}(Mg,Al,Fe^2,Fe^3,Ni,Mn)_{5.4}(Si,Al,Cr)_4O_{10}(OH)_{7.97}$

\#27 Webster, North Carolina (anal. by Gonyer)

$Ca_{.015}(Mg_{5.03}Al_{.36}Cr_{.27}Fe^2_{.23}Fe^3_{.11}Ni_{.02})(Si_{2.91}Al_{1.09})O_{10}(OH)_{7.99}$

$Ca_{.015}(Mg,Al,Cr,Fe^2,Fe^3,Ni)_{6.02}(Si,Al)_4O_{10}(OH)_{7.99}$

\#24 Erzincan Prov., Turkey

$Ca_{.1}(Mg_{4.75}Cr_{.46}Fe^2_{.1}Fe^3_{.02})(Si_{2.93}Al_{.93})O_{10}(OH)_{8.74}$

$Ca_{.1}(Mg,Cr,Fe^2,Fe^3)_{5.33}(Si,Al)_{3.86}O_{10}(OH)_{8.74}$

\#11 Deer Creek, Wyoming (anal. by Shannon)

$Ca_{.14}(Mg_{5.46}Al_{1.16}Fe^2_{.17})(Si_{3.34}Cr_{.65})O_{10}(OH)_{7.08}$

$Ca_{.14}(Mg,Al,Fe^2)_{6.79}(Si,Cr)_{3.99}O_{10}(OH)_{7.08}$

TABLE IV. X-RAY SPECTROGRAPHIC CHROMIUM CONTENT DERIVED
FROM CHEMICAL ANALYSES AND K_α PEAK INTENSITY

	Cr Peak Intensity	$\%$ Cr_2O_3 Chem. Anal.	$\%$ Cr_2O_3 X-ray Spectrographic
No. 4. Zermatt, Valais, Switz.	1.3	0.10	0.10
No. 3. Chester, Pa.	1.9	0.12	0.12
No. 9. Ogushi, Hizen, Japan	7.1	0.54	0.50
No. 2. West Chester, Pa.	16.6	1.14	1.16
No. 17. U.S.S.R.	29.0		2.22
No. 23. Texas, Pa.	37.1		2.94
No. 27. Webster, N. C.	38.8	3.54	3.08
No. 25. Wood's Mine, Pa.	39.7		3.16
No. 10. Siskiyou Co., Calif.	41.9	3.40	3.40
No. 21. Bilimbaievsk, Urals	67.3		5.94
No. 24. Erzincan, Turkey	72.4	6.47	6.47
No. 11. Deer Creek, Wyo.	83.0	7.88	7.79

No. 27. Anal. by Gonyer (Ross, 1929).
No. 11. Anal. by Shannon (1920).
No. 9. U. S. National Museum No. 87144.
No. 17. U. S. National Museum No. 103312.
No. 27. U. S. National Museum No. 97548.
No. 23. U. S. National Museum No. R4534.
No. 10. U. S. National Museum No. 104723.
No. 21. U. S. National Museum No. 16261.
No. 11. U. S. National Museum No. 93908.
Nos. 4, 3, 2, 25, and 24 Columbia University Research Collection.

networks. For reasons presented later, all the chromium in #10 and #11 is placed in tetrahedral coordination. In general, it may be seen that chromium chlorites conform to the theoretical chlorite structure, differences being of a minor order. Specimen #24 contains insufficient cations to fill the tetrahedral layer if all of the chromium is octahedral, as is believed to be the case.

X-ray spectrographic values for chromium were taken from an average of a minimum of 7 runs per sample. The same sample and sample holder were used for each determination. An attempt was made to pack each sample to the same degree to eliminate errors in the amount of sample irradiated per unit surface area. The average of the highest consistent set of three values was used, and is reproducible within the limits of error for instrument reproducibility. Table IV gives the chromium peak intensities for all the chlorites considered in this paper, and the corresponding Cr_2O_3 per cent from both chemical analyses and x-ray spectrographic data.

PART II. MINERALOGY

X-ray Powder Analysis

Introduction

The general chlorite structure is shown in Fig. 1. The details to follow, concerning chromium substitution in chlorite, are based on modifications of this model.
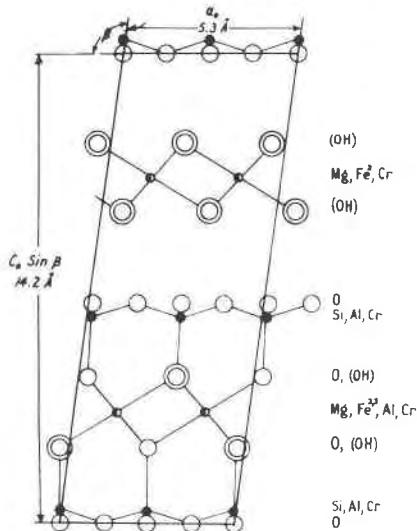

Fig. 1. General chlorite structure. Unit cell in the *a-c* plane (modified after Brindley, 1951, Fig. VI, 4).

Tables and graphs giving *x*-ray data are based on three runs per sample. Sample holders were back-filled to eliminate errors due to sample packing. Curves were obtained at intervals over a two year period to determine the maximum error in reproducibility. An average of three runs was found to yield consistent results, regardless of the time span between runs. A silicon standard was used at each running period to correct for 2θ errors in alignment. All intensity measurements are relative to the strongest line. Since the majority of peaks, with the exception of (020), are sharp, reliable intensities were obtained by subtracting background from peak height. The regularity of the intensity changes, and the ability to utilize *d* value variations to ± 0.1 Å, as illustrated in the graphs, indicate adequate accuracy.

Only chlorites containing more than 1.0 per cent Cr_2O_3 are considered, because lesser amounts have a negligible effect on chlorite structures. Intensity values for (001) reflections below 1 per cent are anomalous

(Fig. 2). The line in Fig. 2 was approximated by sight, because the (001) intensity is affected by ions other than chromium, resulting in a wide scatter of points.

Table V lists *d* values and intensities for chromium chlorites containing more than 1 per cent Cr_2O_3. Chromium content increases to the right. The samples follow the order given in Table IV.
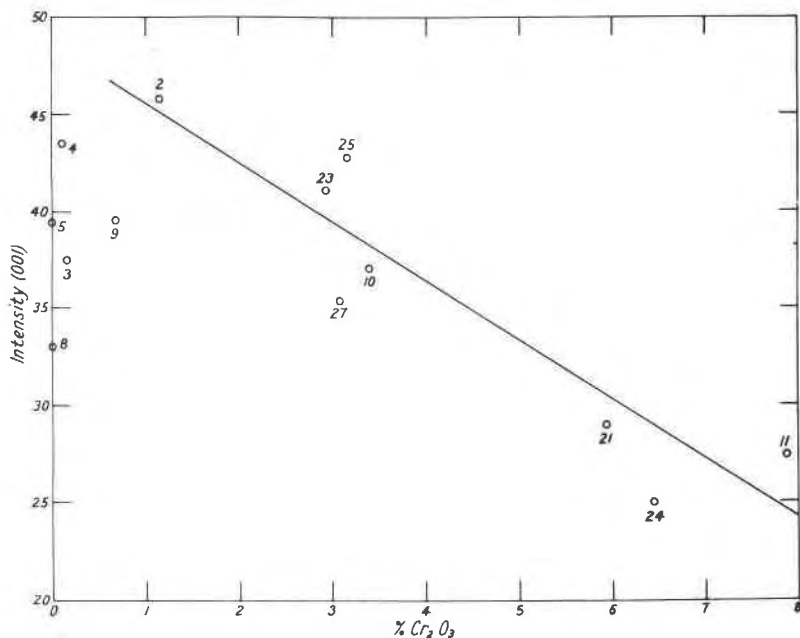
FIG. 2. Variation in chromic oxide content with (001) intensity.

d Spacing—Composition Graphs

Figure 3 represents the effect of chromium substitution on a basal spacing reflection, the (007). Lattice expansion accompanies increasing chromium content. The values suggest an upper and lower curve, the same chlorite samples being located along similar curves for other basal spacings. Chlorites 10, 21, and 11 exhibit lesser expansion with increasing chromium, while chlorites 23, 27, 25, and 24 exhibit greater expansion. Chromium is responsible for this expansion, since it is the only element which varies directly and consistently with *d* values. Although aluminum generally decreases as chromium increases, the relation is irregular. Calcium also increases slightly with chromium (Table I), but

TABLE V. INTERPLANAR SPACINGS AND INTENSITIES

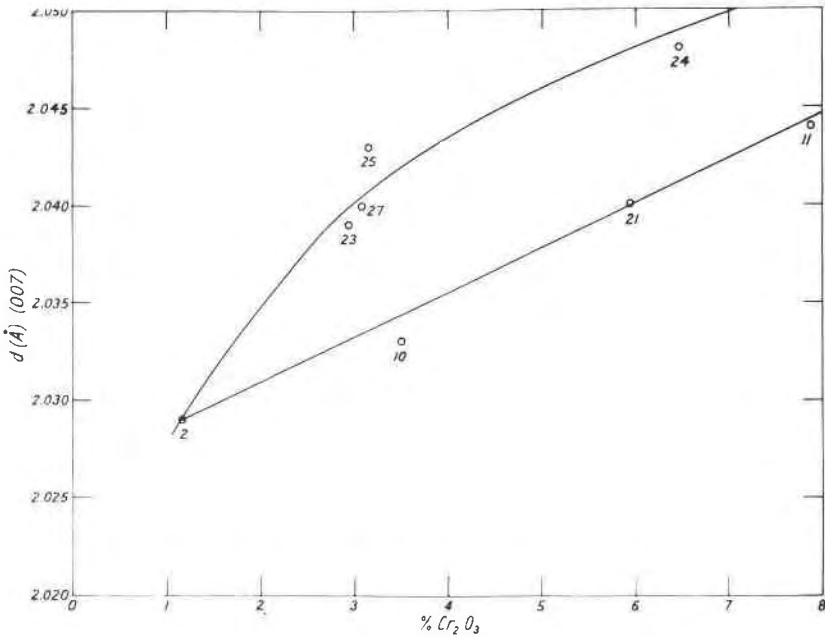| (hkl)	#11 d(A)	#11 Int.	#24 d(A)	#24 Int.	#21 d(A)	#21 Int.	#10 d(A)	#10 Int.	#25 d(A)	#25 Int.	#27 d(A)	#27 Int.	#23 d(A)	#23 Int.	#17 d(A)	#17 Int.	#2 d(A)	#2 Int.
001	14.15	27.4	14.15 7.90	25.0 1.4	14.13	29.0	14.15	37.0	14.17 7.88	42.8 1.9	14.13	35.3	14.10 7.72	41.1 1.9			14.10	45.7
002	7.12	97.6	7.14	100.0	7.11	96.2	7.11	95.2	7.12	95.7	7.11	100.0	7.09	97.0	6.99	99.8	7.083	96.7
003 020	4.756 4.600	99.5 3.8	4.774 4.595	92.4 2.6	4.757 4.589	97.3 5.8	4.741 4.581	92.6 2.0	4.762 4.595	98.8 2.6	4.749 4.604	97.7 3.4	4.746 4.592	97.5 3.0	4.525	2.6	4.727 4.585	87.8 6.0
004	3.572	89.6	3.964 3.589	1.2 90.7	3.951 3.570	2.1 86.3	3.931 3.561	2.0 93.5	3.951 3.573	1.9 89.9	3.943 3.567	1.4 97.7	3.951 3.564	1.8 86.7	3.507	93.5	3.921 3.549	1.3 97.3
005	2.857	22.9	2.868	22.4	2.855	22.8	2.847	24.9	2.858	25.3	2.852	28.4	2.851	24.8	2.602	3.1	2.841	25.0
$131, 20\bar{2}$ $13\bar{2}, 201$	2.581 2.539	3.0 5.4	2.585	1.4	2.585 2.541	3.5 7.1	2.583 2.538	5.7 9.3	2.583 2.539	3.2 5.3	2.577 2.539	2.8 3.8	2.578 2.538	2.7 6.2	2.475	8.0	2.580 2.539	5.6 9.3
$132, 20\bar{3}$ $006, 133$	2.441 2.381	4.0 3.7	2.442 2.387	1.2 5.8	2.443 2.380	5.5 4.0	2.440 2.377	7.2 4.1	2.442 2.382	5.0 3.2	2.442 2.380	3.7 2.6	2.439 2.379	4.9 3.4	2.338	8.2	2.435 2.376	7.7 4.9
$20\bar{4}, 133$	2.328 2.260	1.4 2.8			2.261	3.1	2.322 2.260	2.0 3.3	2.262	2.1	2.261	2.2	2.261	2.6	2.112	2.1	2.257	3.3
007 $204, 13\bar{5}$	2.044 2.008	7.1 6.9	2.048 2.015	6.7 2.8	2.040 2.008	6.9 8.2	2.033 2.003	7.1 7.9	2.043 2.009	6.3 6.6	2.040 2.006	6.8 5.2	2.039 2.006	5.6 7.7	1.924	6.4	2.029 2.001	7.4 10.4
$20\bar{6}, 135$ 136 215	1.889 1.832 1.790	2.6 2.4 1.1	1.893 1.793	0.7 0.9	1.889 1.832 1.789	2.1 3.0 1.1	1.883 1.825 1.803	3.2 2.9 1.5	1.888 1.830 1.782	2.7 2.5 0.8	1.888 1.830 1.805	1.9 1.9 0.8	1.886 1.829 1.782	2.5 2.7 0.8	1.754	3.8	1.880 1.821 1.785	3.8 3.1 1.6
300 $20\bar{7}, 136$ $206, 13\bar{7}$	1.728 1.671	0.9 1.5	1.724 1.674	1.3 3.6	1.725 1.668	1.0 1.6	1.711 1.666	1.3 1.8	1.738 1.724 1.666	0.8 0.8 1.6	1.730 1.714 1.667	0.9 0.9 1.4	1.733 1.721 1.667	1.2 1.1 1.4	1.600	2.4	1.722 1.660	1.2 2.0
208, 137 060	1.573 1.536	5.6 3.4	1.567 1.538	1.8 2.0	1.571 1.538	6.7 4.7	1.569 1.537	6.0 6.1	1.572 1.536	5.8 3.5	1.572 1.538	5.0 3.5	1.571 1.537	6.4 3.0	1.529	3.2	1.564 1.535	7.4 5.7
331, 062	1.503	1.4	1.503	0.9	1.503	1.7	1.501	2.3	1.504	1.3	1.504	1.0	1.502	1.2	1.462	3.3	1.500	2.3
00.10	1.432	3.4	1.435	3.4	1.428	3.2	1.425	2.8	1.430	2.8	1.427	3.0	1.428	3.2	1.402	2.3	1.419	3.1
$1\bar{3}0, 208$	1.402	5.5	1.408	0.4	1.402	6.3	1.396	5.7	1.400	5.1	1.401	5.1	1.401	5.8			1.393	7.2

Fɪɢ. 3. Variation in chromic oxide content with (007) spacing. The upper curve represents octahedral Cr and the lower curve tetrahedral Cr.

it is present in insufficient amounts to cause the observed shifts. Similarly, iron and the Si/Al ratio show no correspondence.

Variations in the diffraction pattern of a chlorite may be attributed to structural and/or chemical variations. Polytypic (stacking) variations such as rotations in the $a–b$ plane result in symmetry changes and hence affect the intensity of reflection. However, they cannot be directly responsible for expansions of basal spacings as long as the mineral is tri-octahedral; i.e., as long as all possible atomic positions are filled. Thus the rotation or shift of succeeding layers does not affect the position of reflection, although it does affect the reflecting power from atomic planes.

The other way in which the expansion of atomic planes may result, if the unit cell structure and degree of crystallinity remain the same, is by varying the position of substitution of one or more cations, in this case, chromium. A comparison of the d values in Table V shows that the fundamental structure remains unchanged. Variations in degree of crystallinity affect peak intensities and peak shapes, but not their position.

Two different sites are available, tetrahedral and octahedral, corresponding to silicon and magnesium positions respectively (Fig. 1).

The substitution of aluminum for silicon contracts the lattice (Brindley, 1951, Fig. VI-7), or conversely, a high Si/Al ratio will expand it. The substitution of aluminum results in an excess negative charge on the tetrahedral layer. This resulting charge imbalance on the tetrahedral layer may be compensated by substitution of ferric iron in the octahedral layer, tending to draw the brucite and talc layers closer together. Here, however, the irregularity of the change in the Si/Al ratio (Tables I and III) indicates that the consistently regular d value changes cannot be due to silicon-aluminum substitutions.

Cr^3 has the same ionic valence as Al^3, but its ionic size is slightly larger. As a result of this increase in size, the substitution of chromium for aluminum in the tetrahedral position would be expected to expand the lattice. In the case of aluminum substitution for silicon, the lattice contracts, because of a local charge imbalance, but the substitution of the somewhat larger Cr^3 ion will expand the lattice only slightly beyond that caused by substitution of an equivalent amount of aluminum, because there is no change in charge. The lower curve in Fig. 3 illustrates such a small linear increase.

The substitution of a trivalent ion, such as chromium, for a divalent ion, such as magnesium, in the octahedral layer creates a greater than normal positive cation charge on this layer. This may be compensated by increasing the amount of $(OH)^-$, or by substituting more aluminum for silicon in the tetrahedral layer. Since the Si/Al ratio generally increases with increasing chromium content, this cannot be a factor in restoring charge balance. A large part of the imbalance is probably made up by the substitution of $(OH)^-$. For example, #24 contains the greatest amount of $(OH)^-$ (Table I). It is significant that this sample exhibits the greatest expansion for the highest Cr_2O_3 percentages. The high Si/Al ratio in the tetrahedral layer, in conjunction with increased chromium in the octahedral layer, results in increased positive cation charge for these cation positions. In such a situation, these two layers tend to expand, because the charge binding the two layers is weak. Because of the nearly equal ionic radii of chromium and magnesium, chromium can be expected to fit easily into this octahedral position. Since there is little change in the sizes of the substituting ions, expansion can be attributed to local charge imbalances which are compensated over a large number of unit cells by substitutions which tend to maintain electrical neutrality. As a result of this chromium substitution, a larger lattice expansion would be expected for octahedral chromium than for tetrahedral chromium. The upper curve in Fig. 3 would then represent octahedral chromium chlorite. Plots for (004), (005), (006), (13$\bar{5}$)(204), (062)(331), c_0, and (13$\bar{7}$)(206) against composition have been found to yield graphs which contain the same separation of points as Fig. 3.

Intensity—Composition Graphs

Since two positions of chromium substitution have been suggested, the effects of this substitution will be considered first, postponing a discussion of polytypism.

If there is a difference in substitution position between octahedral and tetrahedral layers, this difference should be observable from (002) intensities, because the degree of phase addition or subtraction for this reflection is a function of the difference in scattering power between
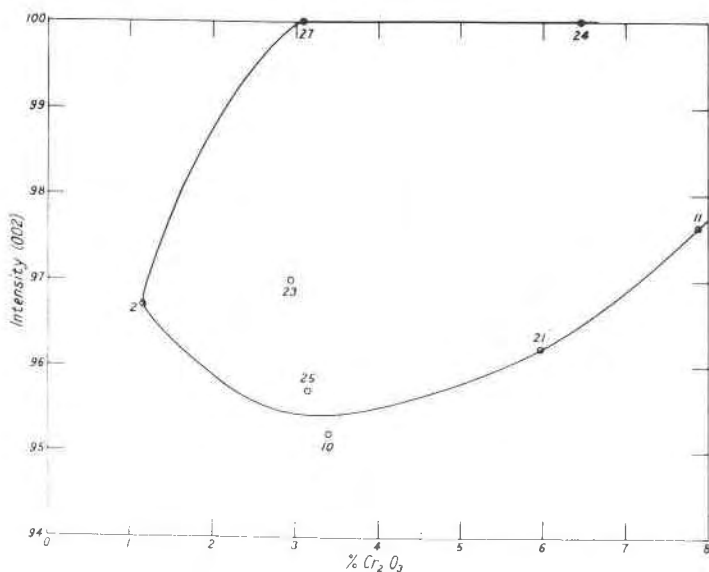

FIG. 4. Variation in chromic oxide content with (002) intensity. The upper curve represents octahedral Cr and the lower curve tetrahedral Cr. No. 23 is anomalous, possibly because of the replacement of octahedral Mg by Ni.

octahedral and tetrahedral sites. Figure 4 illustrates such a separation. The lower curve represents tetrahedral chromium and the upper curve octahedral chromium. Phase relations for normal chlorites indicate that scattering from the octahedral layer is normally greater than that from the tetrahedral layer (See Brindley, 1951, Fig. VI-4). Thus as chromium is substituted in this layer, the larger scattering power of chromium with respect to magnesium increases the intensity of reflection as shown. As chromium substitutes in the tetrahedral layer, the normal situation with greater scattering from the octahedral layer is opposed, so that reflected intensities from these two layers tend to cancel out, and the intensity of reflection decreases. The intensity increase toward #11 is the

result of an unusually large number of octahedral cations, and is not a direct result of tetrahedral chromium substitution.

Sample #23 falls between the two curves in Fig. 4. It may represent chromium substitution in both the tetrahedral and octahedral positions. However, it seems more likely that this particular value is either in error, or anomalous. In all d spacing-composition plots this sample lies on the octahedral chromium curve. Similarly, other intensity-composition plots (Fig. 5) show that it belongs among the octahedral variety. Insufficient material prevented a complete chemical analysis, so that structure factor
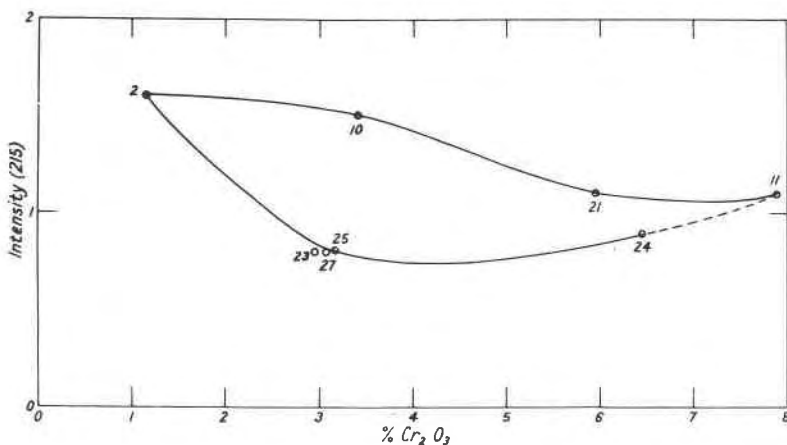

Fig. 5. Variation in chromic oxide content with (215) intensity. The upper curve represents tetrahedral Cr and the lower curve octahedral Cr.

calculations were not possible. X-ray spectrographic data do show that #23 contains considerably more nickel than any of the other samples. Figure 7 shows that its index of refraction is unusually low. These anomalies may be an expression of the high nickel content.

For the (215) reflection (Fig. 5), both tetrahedral and octahedral substitution will decrease intensity, but the contribution due to tetrahedral chromium will have the least effect, because substitution in octahedral sites is the larger contributor to reflection (see Brindley, 1951, Fig. VI-5). Similar plots for (020) and (060) intensity against Cr_2O_3 per cent result and can be explained in a similar manner.

More important than these qualitative considerations are structure factor (F) calculations from observed intensities, which can be compared with F values determined from the samples with a known chemical composition. Table VI gives such a comparison for samples #2, #10, #11, and

#24 for the (001), (002), (003), (004), and (020) reflections. Calculations are based on an "M" type structure which has an a_3 displacement. Coordinates given by Brindley (1951, p. 186) were adjusted to an origin at the octahedral cation position of the talc layer for ease in calculation. The methods of calculation are outlined in Appendix A and B.

For these five reflections, there was only one combination of chromium and iron positions which would satisfy the F order obtained from observed intensities. This data verifies the previous qualitative observations that curves containing #2 and #24 represent octahedral chromium,
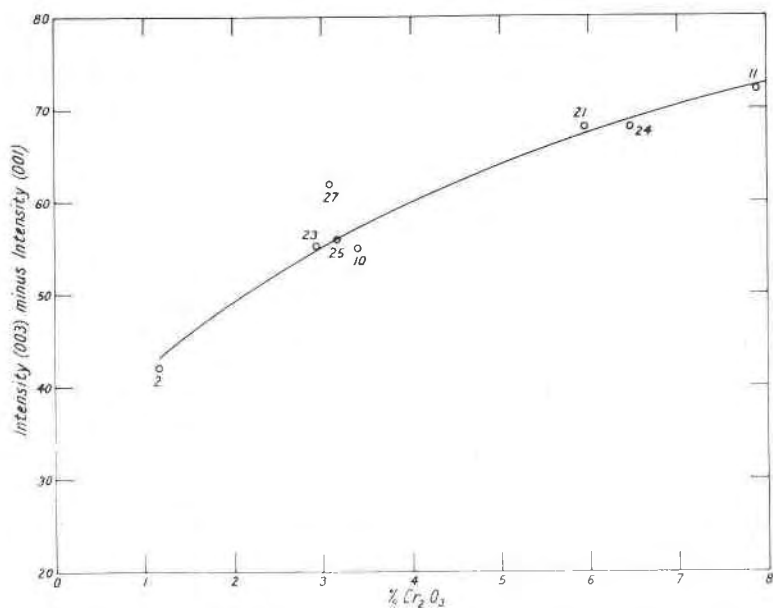

FIG. 6. Variation in chromic oxide content with (003) intensity minus (001) intensity.

and curves containing #10 and #11 represent tetrahedral chromium. In addition, the best fit of theoretical and observed values is obtained when octahedral chromium is placed in the brucite layer, and when the total iron content is divided between the talc and brucite layers. In three instances out of four, the majority of the iron is talc-octahedral. It is interesting to note that plus three chromium, substituting in the octahedral brucite position, is as far removed from the tetrahedral silicon position as the structure permits. Since there is less aluminum than is normally present in Fe-Mg chlorites, the tetrahedral position has a relatively higher positive charge. Chromium would be expected to substitute
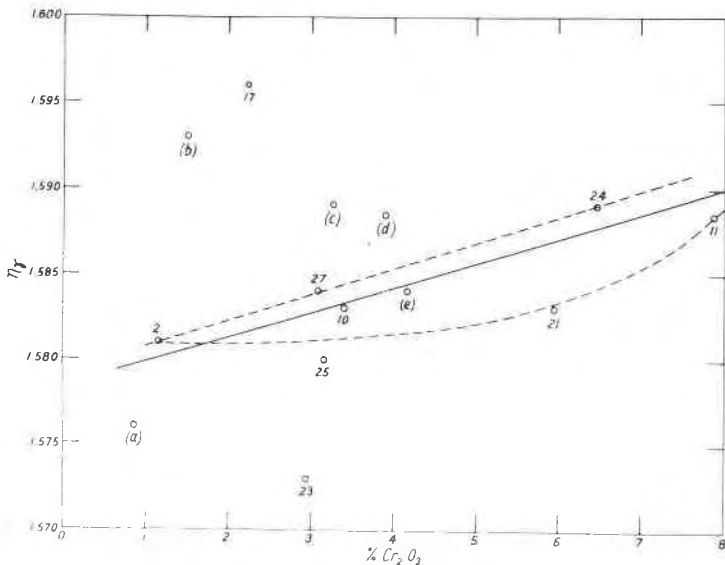
Fɪɢ. 7. Variation in chromic oxide content with gamma index of refraction. Lettered points represent published values, and numbered points represent chlorites studied in this report.

No. 23 is anomalous probably because of the presence of Ni. The upper dashed curve represents octahedral Cr, and the lower curve tetrahedral Cr.

as far away as possible. Slight adjustments were made for the large $(OH)^-$ content of #24, and for the $(OH)^-$ deficiency of #11 (see Table III).

Considering that certain assumptions have been made concerning the structure, the agreement is good. Theoretical F values are very close to those given by Brown (1955) for Fe-Mg chlorite. Garrido (1949) lists comparisons for a chromium chlorite containing $b_0/3$ and $2b_0/3$ shifts with similar discrepancies between theoretical and observed values.

From a consideration of planes whose intensities are unaffected by positional chromium substitution, the amount of Cr_2O_3 may be determined for any chromium chlorite. One of the most accurate of these is the plot of (003) intensity minus (001) intensity against Cr_2O_3 per cent (Fig. 6). The negative F of (003) and the positive F of (001) cancel out positional differences, yielding a straight-line curve.

Stacking variations and lattice displacements (polytypism and polymorphism, respectively) have been mentioned as another mechanism affecting the intensity of reflection. An a_1 shift shift perpendicular to b would not affect intensities to a large extent, nor would it be a continuous

function of chromium content. A similar reasoning holds for a_2 and a_3 shifts. Furthermore, although #24 contains successive 120° rotations, #10 is a normal chlorite without structural displacements (personal communication, Hugo Steinfink), thus indicating that such variation is not the primary cause of observed intensities. However, a consideration of polytypic forms might well yield a closer agreement between theoretical and observed F values.

<center>X-RAY SINGLE CRYSTAL ANALYSIS</center>

Laue Photographs

Laue photographs were taken of samples #17, 21, 10, 24 and 11. Because of a lack of good crystals, the photographs are generally streaked with diffuse or multiple spots. The photographs of #10, #21, and #24 are reproduced in Plate I. Their maximum symmetry is monoclinic. Differences in structure and composition result in differences in intensities for planes with the same index, and in different relative placement of spots and streaks. Sharp spots as in #24 represent well crystallized material. Extreme thickness of the crystal may result in diffuse spots (Schiebold, 1944), and is probably a contributing factor in these photographs. Double or triple spots may be produced in several ways. Lonsdale (1945) notes that double spots result if white radiation contains a strong characteristic component. However, this collimating system has given sharp spots (Plate I, #24), and hence doublets would seem to have a crystallographic origin. Schiebold (1944) reports a similar phenomenon caused by inhomogeneous crystal distortion. Cleavage flakes with such distortions are expected in chlorite crystals. Multiple spots may also be produced by differential absorption or by a mosaic crystal surface (Lonsdale, 1945). The triple spots of #24 might be the result of successive 120° rotations of the 14 Å unit cell, requiring three such rotations to form a repeatable unit cell. If these rotations were not exactly coincident, then reflections from each of the three positions would appear. Maguin (Plate VIII, 1928) shows a Laue photograph of biotite which has a similar tertiary symmetry and which he ascribes to orientations of $+120°$ and $-120°$. He states that chlorites also show this feature. Rotations of this type have been described by Brindley, Oughton, and Robinson (1950). Streaks are probably the result of diffuse reflections where $k \neq 3n$, and hence are most prominent in the b direction.
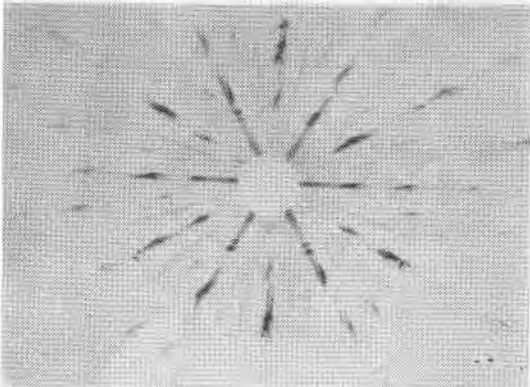
Unexplained hatchet-shaped spots are typical of #10. Good reflections are almost non-existent. #24 exhibits pseudotrigonal symmetry which is expressed surficially by "trigonal prisms" around the c axis. Since a solid solution of one kind of atom in the lattice position of another may yield diffuse spots (Lonsdale, 1945), the greater diffuseness in
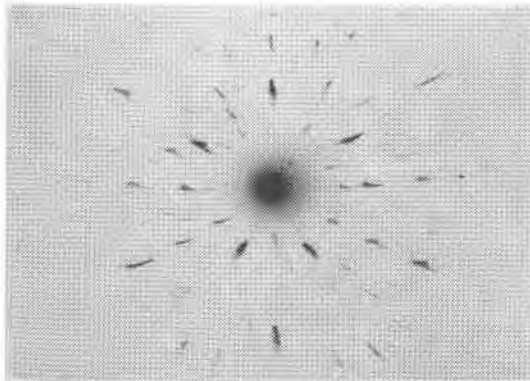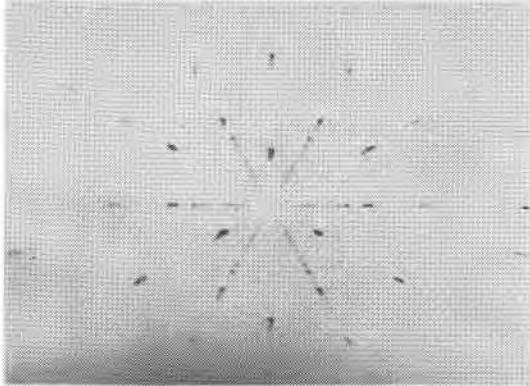
PLATE I. Laue Photographs.

TABLE VI. COMPARISON OF OBSERVED AND THEORETICAL
STRUCTURE FACTOR CALCULATIONS

Sample	Intensity	F-observed	F-theoretical	Cr*	Fe*
(001)					
24	25.0	4.0	50	Brucite	$\frac{2}{3}$ Talc
11	27.4	4.3	52	Talc-Tet.	$\frac{2}{3}$ Brucite
10	37.0	5.1	56	Talc-Tet.	$\frac{2}{3}$ Talc
2	45.7	5.5	59	Brucite	$\frac{2}{3}$ Talc
(002)					
10	95.2	15.7	79	Tet.	—
2	96.7	15.8	89	Oct.	—
11	97.6	15.9	91	Tet.	—
24	100.0	16.1	94	Oct.	—
(003)					
2	87.8	22.9	$-$ 86	Brucite	$\frac{2}{3}$ Talc
24	92.4	23.5	$-$ 90	Brucite	$\frac{2}{3}$ Talc
10	92.6	23.6	$-$ 91	Talc-Tet.	$\frac{2}{3}$ Talc
11	99.5	24.3	-102	Talc-Tet.	$\frac{2}{3}$ Brucite
(004)					
11	89.6	31.2	147	Tet.	—
24	90.7	31.2	147	Oct.	—
10	93.5	32.0	153	Tet.	—
2	97.3	32.4	159	Oct.	—
(020)					
24	2.6	4.1	91	Oct.	—
11	3.8	4.9	92	Tet.	—
2	6.0	6.4	96	Oct.	—
10	7.0	7.0	99	Tet.	—

* Brucite: brucite layer.
  Talc: talc layer.
  Tet.: tetrahedral position.
  Oct.: octahedral position.

samples #10 and #21 may be the result of chromium substitution for aluminum in the tetrahedral position, which is not so well suited to ions as large as chromium.

In general, the Laue method is not sufficient for detailed differentiation among chromium chlorites, but it does illustrate that structural variations may be present.

Rotation and Precession Data

Samples #10 and #24 were given to Dr. Richards A. Rowland, Shell Development Company, who kindly offered to have single crystal photo-

graphs taken as an aid in determining structure. Data presented here are from one rotation and several precession photographs taken by Dr. Hugo Steinfink.

Characteristic streaking, such as that found on Laue photographs, indicates that $k \neq 3n$. Complete streaking would indicate a complete randomness of $1/3$ b shifts. However, there are some spots present along $k \neq 3n$ layers in addition to the streaking, which indicates that the $1/3$ b shifts have a preferred sequence of displacements. These spots occur at integral values of l and can be seen to subdivide the c spacing into three equal divisions, indicating a tripling of the normal 14 Å unit cell spacing. Thus the true height of a unit cell in the c direction is actually 3×14.3 Å or about 43 Å.

Although the true intensities of the spots along $k = 2$ are masked by streaking, they appear to be the same on both $(0kl)$ and $(0\bar{k}l)$, suggesting that the sample is monoclinic. A similar crystal, Brindley's "D" (Brindley, Oughton, and Robinson, 1950), is interpreted as triclinic on the basis of differing intensities for positive and negative indices.

If the unit cell is then taken as 43 Å, there will be an extinction of $(00l)$ spots for which $l \neq 3n$, as the precession photographs show, implying that the c axis of a pseudo unit cell 9×14 Å acts like a 3_1 screw axis. A similar type of pseudo unit cell for the 14 Å variety (normal) of 3×14 Å (orthohexagonal cell) may be constructed. Such a structure means that the stacking of one complete chlorite layer occurs so that each succeeding layer is rotated 120° and then placed on top of the previous layer.

Single crystal photographs of #10 from Siskiyou County contain sharp spots for $k \neq 3n$, indicating a normal well ordered structure. Thus, in one case, the substitution of tetrahedral chromium resulted in a stable 14 Å unit cell, while the octahedral substitution of chromium (#24) resulted in a layer rotation. In the latter instance, a repeatable 14 Å unit cell was not a stable configuration. Additional data from differential thermal analyses supports the hypothesis that polymorphism, unit cell stability, and positional substitution may be inter-related.

OPTICAL PROPERTIES

General Characteristics

Table VII summarizes the optical properties of the nine chlorites discussed. Changes in refractive indices and optic sign will be considered separately. Column 3 shows that there is no consistent change in birefringence with chromium content, although Winchell (1936) has suggested that it might decrease with increasing chromium. The following are additional published values supporting this conclusion:

Sample	% Cr_2O_3	Birefringence	Reference
Newcastle, Calif.	1.5	.012	Shannon (1920)
Patevi, Togo	1.84	.004	Orcel (1927)
Patevi, Togo	4.18	.005	Orcel (1927)
Mt. Albert, Quebec	3.3	less than .010	Osborne and Archambault (1948)
Sweden	13.46	.004	DuRietz (1935)

The accuracy of DuRietz' data is questionable, since the optic sign and indices of refraction do not correspond to the stated chromium content, according to the relation in Fig. 7. The birefringence in Table VII is the difference between the alpha and gamma indices of refraction.

Column 5 suggests that there is no direct correspondence between 2V and chromium content. As in the Fe-Mg chlorites, this angle is generally 10° or less, although Miller (1953) reports a kammererite from Webster, North Carolina containing 3.9 per cent Cr_2O_3 and a 2V of 20°.

In general, chromium chlorites range from colorless or light green to pale pink and violet-pink as chromium increases (column 6). Axial colors are occasionally present.

Pleochroism and absorption tend to increase with increasing chromium (column 7).

Interference colors (column 8) show that chlorites low in chromium have normal first order gray birefringence, while those containing 3 per cent or more Cr_2O_3 exhibit anomalous blue or yellow. Anomalous first order red is characteristic of #24.

Habit (column 9) is commonly irregular to pseudo-hexagonal, viewed on basal plates. Basal sections of #24 are pseudo-trigonal.

Several of the chlorites exhibit additional features of note. Sample #24 has been divided into two types, I and II, on the basis of differing indices of refraction. Type I is not noticeably pleochroic and has lower indices than type II. Type II may represent a higher chromium content. Crystals of #24 taper to a point in the *c* direction and basal sections make internal angles of 120°. Sample #21 has been divided into two types on the basis of differing optic signs. When optically negative, the indices are slightly higher than when optically positive. The optically positive material predominates.

Optic Sign as a Function of Polarizability

The change in optic sign from positive at low Cr_2O_3 percentages to negative at high percentages is dependent on the degree to which the electric vectors of light waves passing through the mineral are additive. This addition is dependent upon the geometry of ionic groups within the mineral structure. Three types of geometrical shapes can be considered: spherical, rod-shaped, and flat or planar. Layer lattices, to which

TABLE VII. CHROMIUM CHLORITE OPTICAL PROPERTIES

No.	Indices of Refraction ±.002			Birefringence ±.002	Optic Sign	2V	Color	Absorption and Pleochroism	Interference Colors	Habit	%Cr$_2$O$_3$
	α	β	γ								
2	1.577—	1.578—	1.581	.004	Biaxial (+)	5–25	colorless to pale green	pale green parallel to N-S nicols	gray	irregular	1.14
17	1.590—	1.590—	1.596	.006	Biaxial (+)	0–18	colorless to pale pink	absent	gray	pseudo-hexagonal	2.2
23	1.568—	1.569—	1.573	.005	Uniaxial to Biaxial (+)	0 to 10	colorless	absent	rarely blue	irregular	2.9
27	1.580—	1.580—	1.584	.004	Uniaxial to Biaxial (+)	0 to 10	X, Y-colorless, pink, blue Z—colorless or yellow	blue to yellow	yellow to rarely blue	pseudo-hexagonal	3.08
25	1.573—	1.574—	1.578	.005	Uniaxial to Biaxial (+)	0 to 10	colorless to pale pink and bluish	absent	blue and yellow	rarely pseudo-do-hexagonal	3.2
10	1.579—	1.580—	1.583	.004	Uniaxial to Biaxial (+)	0 to 30	colorless	absent	blue and yellow	rarely pseudo-do-hexagonal	3.4
21-I	1.580—	1.581—	1.583	.003	Biaxial (+)	0 to 15	colorless to pale pink	absent	blue and yellow	pseudo-hexagonal	5.9
II	1.580—	1.583—	1.584	.004	Uniaxial to Biaxial (−)	0 to 8	as above	absent	as above	as above	
24-I	1.582—	1.586—	1.586	.004	Biaxial (−)	0 to 10	I—pale pink	absent	blue and red	pseudo-trigonal	6.47
II	1.584—	1.588—	1.589	.005	Biaxial (−)		II-X—light pink YZ—violet pink	yellow to pink			
11	1.583—	1.588—	1.589	.006	Biaxial (−)	8	violet pink	X—pale red YZ—dark red	blue to yellow	pseudo-hexagonal	7.88

the chlorites belong, are planar. Their symmetrical ionic arrangement because of the framework structure of the SiO_4 tetrahedra and MgO octahedra, result in a low birefringence, so that their interference colors are almost nil, approaching isotropism.

As a result, substitution in either or both tetrahedral and octahedral positions changes polarizabilities and may also change the optic sign. Light passing through a crystal encounters this directional character of the ionic groups and is consequently polarized. Light vibrating along strongly planar groups will show a strong negative birefringence, with high indices for vibration directions parallel to the planes of the plates, and a low index for light vibrating normal to this direction (Hartshorne and Stuart, 1950). If the ionic groups are still parallel but more rod-shaped, or if they are planar but no longer parallel to each other, then a strong positive birefringence will result (Evans, 1952, p. 272).

Normally chlorites will be slightly positive. However, as chromium is substituted for Si-Al in the tetrahedral layer, and for magnesium in the octahedral layers, these groups increase in planar character and parallelism, and thereby increase their optically negative character. The point at which chlorite changes from optically positive to negative is the point at which the indicatrix is no longer triaxial, changing from an optically positive ellipsoid to one that is negative. Chlorite #21 represents a close approximation to this situation. To the left of the change in optic sign in Fig. 7, positive birefringence tends to increase, while to the right, toward the higher indices and chromium content, negative birefringence tends to increase (Table VII).

The inter-relationship between x-ray analysis and optical studies may be seen to be a function of polarizability, which in turn is dependent upon variations in charge distribution accompanying the substitution of chromium. The greatest effect on optical properties results from octahedral chromium substitution, because substitution of the widely differing chromium ions for magnesium has a greater effect on the planar character of the ionic groups, while the more nearly similar chromium and aluminum produce less significant changes. X-ray data also suggested that octahedral chromium produced more marked effects on lattice spacings and intensities.

Effects of Chromium on Indices of Refraction

Figure 7 is a plot of Cr_2O_3 per cent against the gamma index of refraction. Alpha and beta show similar relations. The solid line curve is considered to be relatively accurate between 3 and 8 per cent, but the wide scatter of points at lower percentages renders this part of the curve inaccurate. The refractive indices of points 2, 17, 23, 25, 10, 27, 21, 24, and 11

were determined using liquids calibrated with sodium light at approximately 0.005 intervals. With the exception of 17 and 23, these points yield a curve with relatively narrow range. Lettered points representing analyses and determinations by other authors indicate that the results of different workers may vary considerably.

Point *a* is a green chromium chlorite from Togo (Orcel, 1927). Point *b* represents Shannon's analysis of a chromium chlorite from Newcastle, California (1920). Since Cr_2O_3 per cent is often too high because of small inclusions of chromite, this determination is probably either anomalous, similar to 17 and 23, or represents an error in index determination. Point (*c*) is from a Quebec sample, analyzed by Osborne and Archambault (1948). Point (*d*) is only an approximate gamma index, since Miller (1953) only listed beta (1.5855) and a positive optic sign. Point (*e*) represents another specimen from Togo (Orcel, 1927). An additional chromium chlorite not shown on the graph has been reported by DuRietz (1935) with the following properties:

$$n = 1.590$$
optically (+)
13.46% Cr_2O_3

Since no other chromium chlorites with more than 5.9 per cent Cr_2O_3 have been found with a positive optic angle, it would seem that either the sign determination or the chromium analysis is in error.

Point 17, representing the 7 Å chlorite, is not directly comparable to the other 14 Å structures. Similarly, points 23 and 25 appear to be anomalous. The presence of other ions such as Fe, Ni, or Ca is suggested as a source of this discrepancy, since *x*-ray spectrographic analyses show that 23 has a NiO content of approximately 0.4 per cent, and 25 of about 0.1 per cent. All other chromium chlorites contained less than 0.1 per cent NiO. Since the index of refraction increases with polarization, substitution of the smaller Ni^2 ion for the larger Fe^2 would tend to lower the index, the nickel ion being less polarizable.

Effects of Chromium Substitution on Polarizability

The solid line curve in Fig. 7 represents changes in refractive indices with increasing chromium substitution. However, in the light of the *x*-ray evidence presented previously, a better approximation to composition may be obtained by utilizing the effects of polarizabilities on optical properties. In unsymmetrical structures such as the chlorites, polarization of a given ion is determined both by the electric vector of the light wave and by the field which results from polarization of its neighboring ions and ionic groups (Evans, 1952, p. 271). Since "the interaction of

electromagnetic waves and matter arises from the polarization of the electronic structure of the individual atoms by the electric vector of the light waves" (Evans, 1952, p. 270), the index of refraction of a mineral is a function of this interaction, and directly related to polarizability. Refractive indices increase with increasing polarizability, which itself increases with the looseness of the ionic bonding. As a result, substitution of a larger ion with equivalent or smaller valence charge tends to increase the refractive indices. Conversely, the substitution of a smaller ion with equivalent or greater charge tends to decrease refractive indices.

Although there is no charge difference between chromium and aluminum, the ionic radius of chromium is larger than that of aluminum (or silicon). Substitution therefore results in looser bonding, greater polarizability, and hence higher refractive indices. However, since chromium is about 0.12 units larger than aluminum, and since the "overwhelming contribution to the refractivity of any ionic compound is . . . due to the anion" (Evans, 1952, p. 25), this substitution will not increase the refractive indices to a large extent.

The lower dashed curve in Fig. 7 corresponds to this case, in which the indices are increased slightly by chromium substitution into the tetrahedral position. It should be noted that the same chlorites fall on this curve as on the *d* spacing-composition-intensity plots in the previous section, with the exception of the anomalous #23 and #25.

On this theoretical basis, it might be expected that substitution of chromium for magnesium, which has a larger ionic radius and a smaller valence charge than chromium, would decrease the polarizability and hence also decrease the refractive indices. A glance at Fig. 7 immediately reveals that this is not the case. However, if it is remembered that the controlling factor in polarizability and variation in indices of refraction is the quantity and distribution of anions, then the increase in indices may be explained. No 24 has more $(OH)^-$ than any of the other chlorites (Table I). Also contributing to this high index is the low Si/Al ratio, which can be compared with a higher ratio for #11. No. 24 also contains more anion radicals per cation than any of the other chromium chlorites studied. Thus the uper curve in Fig. 7 represents octahedral substitution of chromium, and is controlled by anion variation.

Winchell (1936) and Hey (1954) have both remarked that chromium substitution might increase refractive indices analogous to the increase caused by iron substitution for magnesium. Although there is a small general increase in index, the increase is not due directly to substitution of chromium for magnesium, as in the case of Fe^2 for Mg^2, but is primarily due to the amount of anions (or the cation-anion ratio) accompanying octahedral chromium substitution. In addition, not all of the

chromium chlorites can be explained in this manner alone, since tetrahedrally substituted chromium also exists and increases the indices at a different rate. As a result, no single simple relationship appears to exist between indices of refraction and the chromium content in chlorites.

DIFFERENTIAL THERMAL ANALYSIS

Technique and Description

Powdered samples finer than 120 mesh were heated at 12° C. per minute to record the differential exothermic and endothermic reactions between an alundum standard and the sample. Kaolinite was used as a temperature calibration standard, and a minimum of two runs per sample was averaged. The samples were part of uncontaminated material previously examined by other methods. Representative curves appear in Fig. 8.

One exothermic and two endothermic peaks are consistently present, and an additional exothermic peak at about 350° appears in most of the
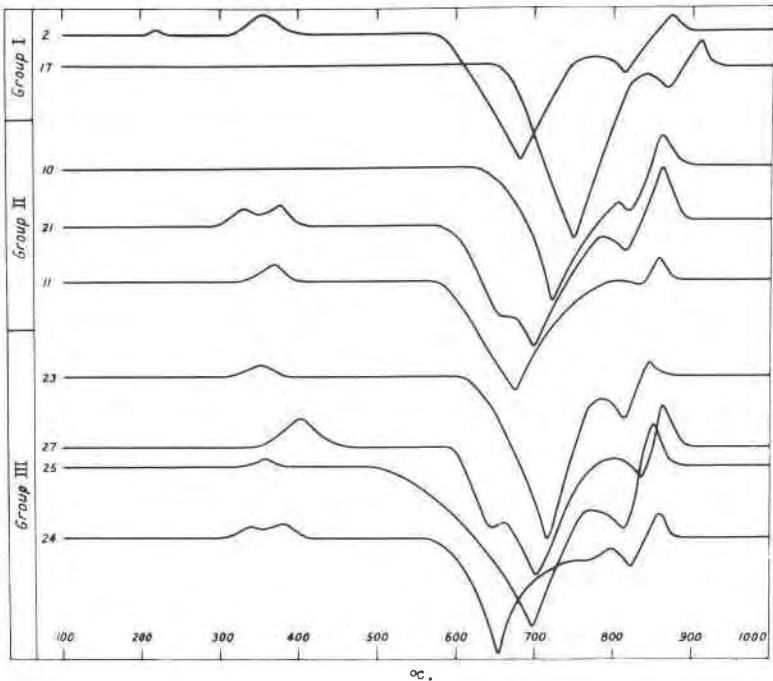

FIG. 8. Differential thermal curves

Group I: Low chromium chlorite (No. 2) and 7A chromium chlorite (No. 17).
Group II: Tetrahedral Cr.
Group III: Octahedral Cr.

samples (Fig. 8). These peaks have been illustrated or mentioned in the literature and will only be summarized here (Ali and Brindley, 1948; Brindley and Ali, 1950; Bradley and Grim, 1951; Nelson and Roy, 1953).

The broad exothermic peak at 350° does not seem to have been noted. A differential thermal curve of penninite given by Ali and Brindley (1948) exhibits a similar peak, but it is not explained. The low temperature of the reaction and the rather broad character of the peak suggest a weak oxidation. No correspondence could be found with chemical composition. No significant changes in x-ray reflections have been noted at this temperature (Brindley and Ali, 1950; Weiss and Rowland, 1956-A and 1956-B).

The first endothermic peak may vary from 550° to 750° C., depending on grain size and chemical composition. Sabatier (1950) reports that single chlorite flakes increase the temperature of this peak to as much as 820° from 620° for the same material finely ground. Increasing substitution of iron for magnesium in the octahedral sites generally decreases this decomposition temperature from a maximum of about 700° to well below 600° C. Brindley and Ali (1950) have correlated this endothermic reaction with the loss of two-thirds of the (OH) in the brucite layer. A one-dimensional electron density Fourier analysis shows a migration of magnesium toward the Si-Al tetrahedra to the position formerly held by the hydroxyls in the brucite layer (Brindley and Ali, 1950).

The second endothermic peak, at about 810° C., represents the completion of dehydration of the chlorite structure, with the loss of two hydroxyls from the brucite layer, and two from the talc layer.

The exothermic peak at about 825° C. accompanies the formation of olivine from chlorite and represents the final destruction of the chlorite lattice. Silicon and magnesium ions must shift slightly to form the olivine structure. If there is more aluminum than an Si/Al ratio of 4 to 1, then difficulties arise and the transition is retarded (Brindley and Ali, 1950). Increasing aluminum tends to raise the temperature of both this exothermic reaction and the previous endothermic reaction. These conclusions are based largely on x-ray data. Differential thermal curves did not show a correspondence between the ease of olivine formation and aluminum content.

General Thermal Characteristics

Three groups of curves in Fig. 8 represent (I) a low chromium chlorite (#2) and the anomalous 7 Å sample (#17); (II) tetrahedral chromium chlorite (#10, #21, and #11); and (III) octahedral chromium chlorite (#23, #27, #25, and #24). The members of each group are arranged in

order of increasing Cr_2O_3 content. Only the endothermic peak between
640° and 750° C. shows a consistent change together with composition.
No systematic variation in the 810° endothermic or 840° exothermic
peaks appears with respect to aluminum content. However, the high
temperatures of these two peaks for #17 indicates difficulty in the olivine
transition, and may be a function of the Si/Al ratio, as proposed by
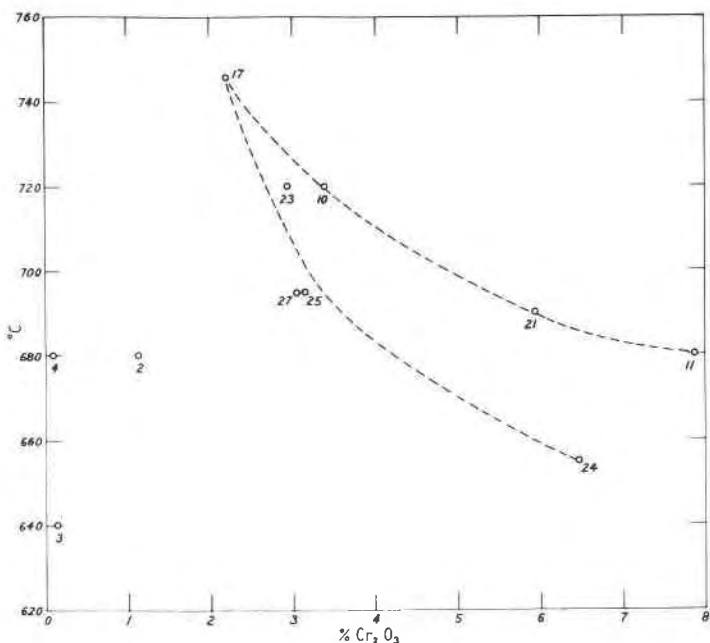Brindley and Ali (1950).

Fig. 9. Variation in chromic oxide content with temperature of decomposition of the
brucite layer. The upper curve represents tetrahedral Cr and the lower curve octahedral
Cr.

The correlation between chromium content and temperature is il-
lustrated in Fig. 9. Two features appear: (1) above 2 per cent, the Cr_2O_3
content increases as the temperature of decomposition of the brucite
layer decreases—this is approximately the same limit above which cor-
respondence with x-ray reflections becomes significant; (2) correlation
with chromium follows two different curves which contain the same
samples as on the previous x-ray and optical curves, differentiating be-
tween tetrahedral and octahedral chromium. In this instance, tetra-
hedral chromium is represented by the upper curve and octahedral by
the lower.

Effects of the Position of Chromium Substitution

From Fig. 9 it appears that the substitution of chromium in the tetrahedral position increases the thermal stability of the brucite layer over the thermal stability for octahedral substitution at the same Cr_2O_3 percentages. It seems likely that tetrahedral substitution, once accomplished, yields a more stable chlorite. Hence although substitution is governed largely by ionic size which usually results in octahedral chromium, the stability of a lattice once formed will depend largely on charge distribution, as long as the substituting ions do not differ greatly in size. Tetrahedral substitution probably represents the replacement of aluminum (and secondarily, silicon) by chromium in Si-O tetrahedra, and hence results in no change in local charge distribution for this position beyond the normal (Fe-Mg) chlorite balance. In the specimens studied, chromium in the aluminum position does not exceed one ion per unit cell. Such a substitution may be indicative of high temperatures, allowing chromium to substitute in the less favorable tetrahedral site. On the other hand, the replacement of Mg^2 by Cr^3, while more common because of their similar ionic sizes, results in a local charge imbalance in the octahedral sites, decreasing the thermal stability of the lattice. Thus octahedral substitution may be indicative of lower temperatures of crystallization because of the greater ease of chromium substitution. It is interesting to note that the two curves converge toward the 7 Å specimen (#17), suggesting that it has been converted to a 14 Å structure, as Nelson and Roy (1953) have reported.

Referring to chromium substitution in chlorite, Roy and Tuttle (1956) state, "the decomposition temperatures are lowered 50 to 100° C. when compared to the pure Al members." From this data, it may be seen that such a lowering of temperature does not necessarily occur. The maximum decomposition temperature for the normal chlorite structure is slightly less than 700° C., while the maximum for chromium chlorite is about 745° C., or nearly 50° C. higher. Only at Cr_2O_3 percentages greater than 4 per cent does the decomposition temperature decrease below that of the pure Al member. As iron is substituted for magnesium, regardless of the amount of aluminum present, the temperature is decreased so that conceivably there could be no difference at all between the chromium and pure aluminum chlorites.

Ionic charge, size, and position of substitution do not completely explain the data, because Fig. 9 represents the decomposition of the brucite layer, which does not contain a tetrahedral position. Yet the substitution of chromium in the tetrahedral position also decreases the thermal stability of the brucite layer. As would be expected, tetrahedral chromium has less effect, since substitution directly into that layer affects that

layer more, and as a result, the octahedral curve is at a lower temperature and has a steeper slope. This can be explained on the basis of local charge imbalances, resulting in decreased bond strength as chromium substitution increases.

The chemical formulas for samples #2, #10, #27, #24, and #11 have been given in Table III. Considering these to be relatively accurate, the following total charge imbalance exists, according to the above sample order, which is arranged according to increasing chromium content: -0.98; -1.49; -0.33; -2.89; and $+2.25$. Qualitatively it may be seen that increasing charge imbalance is roughly parallel to both increasing chromium content and decreasing temperature of decomposition (or decreasing lattice stability). Orcel, Caillere, and Henin (1950) have discussed charge imbalances and noted that they affect the decomposition temperature of the brucite layer. They make an analogy between excess charge on the brucite layer and the role played by potassium in micas. However, they state that the quantity of trivalent elements necessary to compensate for the deficit of charges on the mica (talc) layer (or the excess on the brucite) is insufficient, resulting in a chlorite whose structure approaches that of the expanding chlorites. These local charge imbalances are compensated by substitution of Na, K, or Ca into hexagonal network cavities of the chlorite structure. An excess positive charge might tend to be balanced by an increase in $(OH)^-$. It is significant that calcium content increases with chromium content, tending to balance local charge deficiencies.

The explanation for decreasing decomposition temperature with increasing chromium can be given more accurately than the above approach. If one takes the theoretical number of octahedral cations per unit cell, which is six, and finds the amount by which this differs from the actual case, this difference is then a measure of the degree of charge imbalance in the octahedral position, and should thus be directly comparable to the decomposition temperature of the brucite layer. In the following list, the compensation of charge imbalance by $(OH)^-$ is included:

> #2 . . . 0.62 relative degree of charge imbalance
> 10 . . . 0.57 relative degree of charge imbalance
> 27 . . . 0.03 relative degree of charge imbalance
> 24 . . . 1.41 relative degree of charge imbalance
> 11 . . . 1.71 relative degree of charge imbalance

This list is also in order of increasing chromium content. In order of decreasing stability, according to octahedral cation charge imbalance, this would be:

$$\text{#27—#10—#2—#24—#11.}$$

The observed order from differential thermal data is:

#10—#27—#2—#11—#24.

Numbers 10 and 11 appear to be out of order, if this theoretical picture were to correspond to observed thermal stabilities. However, when one considers that these two samples are the only ones in the above list in which the chromium occupies a tetrahedral site, and that a charge imbalance in the tetrahedral position would have less effect on the more distant brucite layer, then the theoretical picture fits the observed data. Thus, although the actual amount of charge imbalance is not accurate because of limitations such as the chemical analyses, the relative degree of imbalance is accurate and does explain the order of instabilities as observed from the breakdown temperatures of the brucite layer.

Conclusion

If this theoretical picture is correct, and it seems to explain the data as well as support the conclusions from x-ray analyses, then a small total charge imbalance exists on a unit cell which is not compensated by cation or hydroxyl substitution. It seems that substitution of these ions is in such a position as to be nearest the greatest charge imbalance. Since charge imbalances are effective only over short distances, the instability of the lattice is minimized. However, there is a further mechanism which may help to alleviate lattice stress caused by charge imbalances. If rotations or glides of successive unit cells occurred so that positions of charge excesses were placed over charge deficiencies, or nearer to them, greater stability would result. Octahedral chromium should create the most significant imbalances, because a trivalent ion is being substituted for a divalent one. The octahedral chromium chlorite from Erzincan (#24) has just such a rotation of successive layers. On the other hand, as would be expected in a substitution of chromium for aluminum, the tetrahedral California chromium chlorite (#10) has a normal structure without rotations. Thus the structures of two samples of chromium chlorite can be explained as a function of charge imbalance. That this imbalance might be a cause of polytypism and polymorphism in layer lattices should be investigated.

Substitution of chromium in the chlorite lattice results in minor structural variation, since unit cell symmetry is changed by the positioning of the chromium ion. Aluminum is another element which also substitutes in two different coordination sites. Both polymorphism and polytypism are used for structural variations. Polymorphism results in "structures characterized by different lattices" while polytypism is "any possible structural modification which alters the (c) axis dimension of the smallest unit cells referable to . . . lattice types by some multiple

of a single layer . . . without altering the structure in the plane per-
pendicular thereto" (Strock and Brophy, 1955). Polytypism may be
thought of as variations in the stacking sequence along the c direction,
while polymorphism refers to a major symmetry change.

Neither polymorphism nor polytypism accurately describes the
chromium chlorite situation. Since diadochy is the substitution of one
element for another in the same structure, "positional diadochy" could
be used to describe octahedral and tetrahedral chromium substitution.
However, to avoid confusion, with existing nomenclature, perhaps the
term "comorphism" is preferable, to be defined as follows:

the substitution of one element in two different coordination positions in the same mineral
lattice, resulting in a minor structural variation without necessarily changing the unit cell
composition.

PART III. CLASSIFICATION

REVIEW

The nomenclature of chromium chlorite contains many revised species
descriptions. Old terms have been replaced and superseded as new data
has become available and as the basis for mineral classification has
shifted toward an emphasis on internal structures. A brief summary of
the most common names is discussed as a step toward a new classification.

The term "chrome chlorite" has frequently been used to refer to rose-
violet chlorite in order to avoid confusion with the green Fe–Mg chlorites.
The term has also been used for green chlorites containing a maximum
of 2 per cent Cr_2O_3. However, this color composition boundary is in-
distinct. Shannon (1920) reports a pale lavender kammererite from New-
castle, California, averaging 1.53 per cent Cr_2O_3. Pearse (1864) noted a
green chromium chlorite from Lancaster County, Pennsylvania con-
taining 1.967 per cent Cr_2O_3. Orcel (1927) used 2 per cent as the color
composition boundary, while Hey (1954) suggests the term "chrome
chlorite" for samples with less than 4 per cent Cr_2O_3. Hey's preference
for this percentage lies in an analogy with a 4 per cent Fe_2O_3 boundary
often used to separate orthochlorites (largely $MgO+FeO$) from lepto-
chlorites (containing more than 4 per cent Fe_2O_3).

Kammererite is the most widely used and oldest term for rose-violet
chromium chlorite. Dana (Garrett, 1853) first placed it in the pyro-
sclerite group, now believed to be a member of the vermiculite family.
Later he described it as a Cr-variety of penninite (Dana, 1892, 6th ed.)
and used rhodochrome for optically negative kammererite and rhodo-
phyllite for the optically positive variety. Vernadsky (1901), Orcel
(1927), and Hey (1954) use kammererite for a chromiferous variety of
penninite. Since penninite has a higher Si/Al ratio than the other Fe–Mg

chlorites, the definition of kammererite is based on this ratio, rather than on any direct relation to chromium.

In 1852, Dr. F. A. Genth proposed the name rhodophyllite for violet chromium chlorite from Texas, Pennsylvania containing between 4 per cent and 7 per cent Cr_2O_3. Somewhat earlier, the name rhodochrome had been applied to violet chromium chlorite (Smith and Brush, 1853) but without a chemical analysis. When the analysis (from Lake Iktul, Urals) was published, it was found to fall within the Cr_2O_3 range of the Texas rhodophyllite. Smith and Brush then proposed that since the two were identical, rhodochrome had precedence. However, the terms appear to have become somewhat confused, since Dana (1892) differentiated the two on the basis of optic sign and placed both under the kammererite subdivision of penninite.

In 1861, Kokscharow is credited with having proposed the name kotschubeite for an optically positive variety of chrome clinochlore (Melville and Lindgren, 1889).* On the basis of this definition, the distinction between kammererite and kotschubeite is one of aluminum content, analogous to the distinction between penninite and clinochlore respectively. According to the analysis by von Leuchtenberg (Melville and Lindgren, 1889), kotschubeite from Lake Iktul contained 4.09 per cent Cr_2O_3. Thus this locality produced two chromium chlorites, rhodochrome and kotschubeite, containing similar amounts of chromium, but apparently differing in Si/Al ratio. Based on this ratio, Melville and Lindgren used kotschubeite for a California sample containing 11.39 per cent Cr_2O_3. Orcel (1927) concurred that kotschubeite was an optically positive variety of clinochlore. Fisher (1929) stated that kotschubeite had a lower birefringence than kammererite. Hey (1954) used only the terms "chrome-clinochlore" where the Cr_2O_3 content was less than 4 per cent, and "kotschubeite" for chrome clinochlore containing more than 4 per cent.

In summary, it seems that there are by original definition two distinct varieties, kammererite and kotschubeite, based on their Si/Al ratio. Rhodochrome and rhodophyllite are indistinguishable from them. Both optically negative and positive chromium chlorites exist; published Cr_2O_3 percentages range up to 13.5 per cent; and, the Si/Al ratio of penninite to clinochlore represents a minimal variation. Color is not a reliable criterion for classification.

Proposed Nomenclature

The value of any mineralogic classification lies both in its simplicity

---

* The reference which is given as Bull. Acad. St. Petersburg, 1861, p. 369, appears to be incorrect.

and the ease with which it may be applied in the field and laboratory.
Both the Fe–Mg and Cr– chlorite literature is studded with names,
many of them overlapping and most of them subdivided on an arbitrary
basis. In 1950, Orcel, Caillere, and Henin proposed a classification based
primarily on the number of tetrahedral silicon ions, and secondarily on
iron content, the boundaries being arbitrary for the most part. Their
main divisions are as follows:

	Tetrahedral Si
Amesite	2.0–2.2
Prochlorite	2.3–2.8
Clinochlore	2.9–3.5
Pennine	3.5 or greater

Nelson and Roy (1953) largely followed this main division, but reduced
the prochlorite field and added corundophilite between amesite and
prochlorite. Max Hey (1954) also divided the chlorites according to
amount of tetrahedral silicon, using corundophilite, sheridanite, clino-
chlore, and penninite for the relatively iron-free members, but including
many other names for more iron-rich members.

The distinction between one mineral and another should be based
both on crystal structure and chemical composition. When a substitu-
tion series exists in one group, as it does in the chlorites, arbitrary
amounts of cation substitution have little meaning in the construction
of a classification. If there are no structural variations, names applied
to subdivisions should be kept to a minimum. Such a subdivision has
been useful in the Fe–Mg and Si–Al series of chlorite substitutions.

Chromium chlorites present a different problem. The correspondence
between chromium content and structure, evidenced by x-ray, optical,
and differential thermal analyses, begins between 1 per cent and 2 per
cent Cr_2O_3, indicating that below this amount chromium substitution
has little structural effect. Hence, it is proposed that chlorites containing
less than 2 per cent Cr_2O_3 retain the Fe–Mg chlorite nomenclature, adding
"Cr" as a prefix (Group I, Table VIII). At greater than 2 per cent a
significant and recognizable correspondence exists with the chlorite
structure. In addition, there is a distinct separation into octahedral
and tetrahedral types of chromium substitution. Here then, is a struc-
tural variation which will allow a nomenclature based on a measurable
difference—one which is perhaps less arbitrary than previous usages.
The two most commonly used names for chromium chlorite are kam-
mererite and kotschubeite. Their previous distinction, based on optic
sign or Si/Al ratio, has not been consistent nor does it have a fundamental
structural basis. Since the type locality for kotschubeite is Lake Iktul,
Urals, it seems appropriate that the tetrahedral Bilimbaievsk sample

TABLE VIII. CLASSIFICATION OF 14Å CHLORITES

I—Mg—Fe—Cr Chlorite				
Tetrahedral Si	Mg Chlorite	Fe Chlorite		Cr Chlorite—less than 2% Cr_2O_3
		Ortho-chlorite >4% FeO	Lepto-chlorite >4% Fe_2O_3	
2.0–2.5	Corundophilite	Fe corundophilite		Cr corundophilite
2.5–2.8	Prochlorite	Fe prochlorite		Cr prochlorite
2.8–3.1	Clinochlore	Fe clinochlore		Cr clinochlore
3.1 or greater	Penninite	Fe penninite		Cr penninite

II—Chromium Chlorite—more than 2% Cr_2O_3	
Tetrahedral Cr	Octahedral Cr
Kotschubeite	Kammererite

(#21), which is named kotschubeite, be taken to represent the tetrahedral group. Octahedral chromium chlorites, which appear to be more common, have generally been referred to as kammererites. This name is suggested to represent the octahedral group (Group II, Table VIII). "Chromium chlorite" is suggested as a general and field term for pink to rose-violet chlorite.

On the basis of this nomenclature, the 14 Å samples studied would have the following species names:

#2 West Chester, Pa.	Cr-clinochlore
23 Texas, Pa.	kammererite
27 Webster, N. C.	kammererite
25 Woods Mine, Pa.	kammererite
10 Siskiyou County, Calif.	kotschubeite
21 Bilimbaievsk, Urals	kotschubeite
24 Erzincan, Turkey	kammererite
11 Deer Creek, Wyo.	kotschubeite

Chlorites containing both octahedral and tetrahedral chromium may be classified according to the position which contains the majority of chromium. Nomenclature for the 7 Å chlorites has yet to be agreed upon, and hence #17 has not been included in this classification.

SUMMARY

Chromium substitutes into both the octahedral and tetrahedral positions of chlorite. Above 2 per cent chromic oxide content, the former are

termed kammererite, and the latter kotschubeite. This structural variation is referred to as positional diadochy, or comorphism. It is suggested that such positional substitution is related to local unit cell charge imbalances, which in turn may have a causal effect on polytypic variations.

APPENDIX

A. Calculation of F values from observed intensities:

$$F^2 = \frac{I}{(j)\dfrac{1 + \cos^2 2\theta}{2} \cdot \dfrac{1}{2\sin^2\theta\cos\theta} \cdot A(\theta)}$$

where

> F = structure factor
> I = observed intensity
> j = multiplicity factor
> 2θ = Bragg reflection angle
> $A(\theta)$ = absorption factor evaluated from NaCl standard as $1/u$
> > where

$$u = p\Sigma \frac{\text{At. wgt.}}{\text{Tot. wgt.}} \cdot \frac{u}{p}$$

> where

> > p = chlorite density

> > $\dfrac{u}{p}$ = mass absorption coefficient for each element

B. Calculation of theoretical F values

$$F = 8\cos^2 2\pi \frac{h+k}{4}\cos^2 \pi(hx + lz)\cos 2\pi ky$$

expanded using

$$\cos(a + b) = \cos(a)\cos(b) - \sin(a)\sin(b)$$

and

$$\cos^2\theta = \tfrac{1}{2}(1 + \cos 2\theta)$$

$$F = 4\left[1 + \cos\left(2\pi\frac{h}{2}\right)\cos\left(2\pi\frac{k}{2}\right) - \sin\left(2\pi\frac{h}{2}\right)\sin\left(2\pi\frac{k}{2}\right)\right]$$
$$\cdot \left[\cos(2\pi hx)\cos(2\pi lz) - \sin(2\pi hx)\sin(2\pi lz)\right] \cdot \cos(2\pi ky)$$

REFERENCES

ALI, SULTANA Z. AND BRINDLEY, G. W. (1948), X-ray study of thermal transformations in the chlorite mineral, penninite, *Leeds Phil. and Lit. Proc.*, **V,** part II, sci. sect., 109–115.

BRADLEY, W. F. AND GRIM, R. E. (1951), High temperature and thermal effects of clay . . . , *Am. Mineral.*, **36,** 182–201.

BRINDLEY, G. W. AND ALI, SULTANA Z. (1950), X-ray study of thermal transformations in some magnesian chlorite minerals, *Acta Cryst.*, **3,** 25–30.

————, OUGHTON, BERYL M., AND ROBINSON, KEITH (1950), Polymorphism of the chlorites, Part I, ordered structures, *Acta Cryst.*, **3**, 408–416.

———— (edit.) (1951), *X-ray Identification and Crystal Structures of Clay Minerals*, pub. Taylor and Francis Ltd., London, pp. 173–198, 186.

BROWN, GEORGE (1955), The effect of isomorphous substitution on the intensities of (001) reflections of mica and chlorite type structures, *Min. Mag.*, **30**, 657–665.

DANA, E. S. (1892), *System of Mineralogy*, 6th ed., New York, pp. 653–654.

DURIETZ, TORSTEN (1935), Peridotites, serpentines and soapstones of Northern Sweden, *Geol. For. Forh. Stockholm*, **57**, 133–260.

EVANS, R. C. (1952), *An Introduction to Crystal Chemistry*, pub. University Press, Cambridge, pp. 24–25, 270–274.

FISHER, LLOYD W. (1929), Origin of chromite deposits, *Ec. Geol.*, **24**, 691–721.

GARRETT, THOMAS H. (1853), On minerals accompanying chromic iron, *Am. Jour. Sci.* 2nd Ser., **15**, 332–334.

GARRIDO, JULES (1949), Structure cristalline d'une chlorite chromifere, *Bull. Soc. Franc. Min. et Crist.*, **72**, 549–570.

GENTH, F. A. (1852), On rhodophyllite, a new mineral, *Proc. Nat'l. Acad. Sci. Phila.*, **6**, 121–124.

HARTSHORNE, N. H., AND STUART, A. (1950), *Crystals and the Polarizing Microscope*, 2nd ed., publ. Edward Arnold & Co., London, pp. 130–155.

HEY, MAX H. (1954), A new review of the chlorites, *Min. Mag.*, **30**, 277–292.

LONSDALE, K. (1945), The shape of reflections on X-ray single crystal photographs, *Min. Mag.*, **27**, 112–125.

MAUGUIN, CH. (1928), Etude des micas au noyen des rayons X, *Soc. Franc. Min. Bull.*, **51**, 321.

MELVILLE, W. H. AND LINDGREN, W. (1889), Contributions to the mineralogy of the Pacific Coast, *U. S. Geol. Surv. Bull.*, **61**, 11–40.

MILLER, ROSEWALL (1953), The Webster-Addie ultramafic ring, Jackson Cy., Nor. Car. and secondary alteration of its chromite, *Am. Mineral.*, **38**, 1134–1147.

NELSON, BRUCE W. AND ROY, RUSTUM (1953), New data on the composition and identification of chlorites, *2nd National Conference on Clays and Clay Minerals*, Nat'l. Acad. Sci. Pub. #**327**, 335–348.

ORCEL, M. J. (1927), Recherches sur la composition chimique des chlorites, *Bull. Soc. Franc. Min.*, **50**, 75–456.

————, CAILLERE, S., AND HENIN, S. (1950), Nouvel essai de classification des chlorites, *Min. Mag.*, **29**, 329–340.

OSBORNE, F. F. AND ARCHAMBAULT, M. (1948), Chromiferous chlorite from Mount Albert, Quebec, *Roy. Soc. Canada Trans.* Ser. 3, **42**, 61–67.

PEARSE, J. B. (1864), On some minerals of the chlorite group, *Am. Jour. Sci.* 2nd Ser., **37**, 221–225.

ROSS, CLARENCE S. (1929), Is chromite always a magmatic segregation product?, Part II, *Ec. Geol.*, **24**, 641–645.

ROY, RUSTUM AND TUTTLE, O. F. (1956), Investigations under hydrothermal conditions, *Physics and Chemistry of the Earth*, **1**, 166–167.

SABATIER, G. (1950), Sur l'influence de la dimension des cristaux de chlorites sur leurs courbes d'analyse thermique differentielle, *Soc. Franc. Min. Crist. Bull.*, **73**, 43–48.

SCHIEBOLD, E. (1932), *Methoden der Kristallstrukturbestimmung mit Rontgenstrahlen*, Akad. Verlag. M.B.H. Leipzig, pub. J. W. Edwards, 1944, pp. 137, 144.

SHANNON, E. V. (1920), Analyses and optical properties of amesite and corundophilite from Chester, Mass. and of chromium-bearing chlorites from Calif. and Wyo., *U. S. Nat'l. Museum Proc.*, **58**, 371–379.

SMITH, J. LAWRENCE AND BRUSH, GEORGE J. (1853), A reexamination of American minerals, *Am. Jour. Sci.* 2nd Ser., **16,** 47–48.

STROCK, L. W. AND BROPHY, V. A. (1955), Synthetic ZnS polytype crystals, *Am. Mineral.*, **40,** 94–106.

VERNADSKY, W. J. (1901), Zur theorie der silicate, *Zeit. Krist.*, **34,** 37–66.

WEISS, E. J. AND ROWLAND, R. A. (1956-A), Oscillating heating *X*-ray diffractometer studies of clay mineral dehydroxylation, *Am. Mineral.*, **41,** 117–126.

——— (1956-B), Effect of heat on vermiculite and mixed layer vermiculite-chlorite, *Am. Mineral.*, **41,** 899–914.

WINCHELL, A. N. (1936), A third study of chlorite, *Am. Mineral.*, **21,** 642–651.